EuroIntervention 2022;18:203-212 published online ahead of print March 2022

Coronary access after transcatheter aortic valve replacement in bicuspid versus tricuspid aortic stenosis

Fei Chen[1], MD; Kaiyu Jia[2], MD; Yijian Li[1], MD; Tianyuan Xiong[1], MD; Xi Wang[1], MD; Zhongkai Zhu[1], MD; Yuanweixiang Ou[1], MD; Xi Li[1], MD; Xin Wei[1], MD; Zhengang Zhao[1], MD; Qiao Li[1], MD; Sen He[1], MD; Jiafu Wei[1], MD; Yong Peng[1], MD; Yuan Feng[1], MD; Mao Chen[1]*, MD, PhD

1. Department of Cardiology, West China Hospital, Sichuan University, Chengdu, China; 2. West China School of Medicine, Sichuan University, Chengdu, China

This paper also includes supplementary data published online at: https://eurointervention.pcronline.com/doi/10.4244/EIJ-D-21-00970

KEYWORDS

- aortic stenosis
- coronary access
- MSCT
- TAVR

Abstract

Background: It is unknown whether there are differences in coronary access after transcatheter aortic valve replacement (TAVR) between bicuspid and tricuspid anatomy.

Aims: Our aim was to investigate coronary access after TAVR using a self-expanding transcatheter heart valve (THV) in bicuspid versus tricuspid aortic valves (BAV vs TAV), based on CT simulation.

Methods: A total of 86 type 0 BAV, 70 type 1 BAV, and 132 TAV patients were included. If the coronary ostium faced the sealed parts of the THV or the tilted-up native leaflet (NL), this was defined as THV- or NL-related challenging coronary access, respectively. If coaxial engagement was not allowed due to interference from the unwrapped frame, THV-related complex coronary access was defined.

Results: The incidence of THV-related challenging coronary access was 21.2% for the left coronary artery (LCA) and 17.7% for the right coronary artery (RCA), and type 0 BAV patients encountered fewer THV-related challenging LCA access than their TAV counterparts (OR 0.42, 95% CI: 0.20 - 0.89). NL-related challenging coronary access was observed in 3.1% for LCA and 1.4% for RCA, and THV-related complex coronary access was identified in 5.9% for LCA and 17.0% for RCA; however, no significant differences were found among groups. The proportion of optimal fluoroscopic viewing angles suitable for guiding LCA engagement was similar among groups (64.0% vs 70.0% vs 62.1%), but those suitable for guiding RCA engagement were significantly higher in the type 0 BAV group (31.4% vs 4.3% vs 9.1%).

Conclusions: Coronary access may be challenging or complex in a significant proportion of both BAV and TAV patients after TAVR. Type 0 BAV anatomy may be more favourable for post-TAVR coronary access.

**Corresponding author: Department of Cardiology, West China Hospital, Sichuan University, No.37 Guoxue Alley, Chengdu 610041, PR China. E-mail: hmaochen@vip.sina.com*

SUBMITTED ON 05/11/2021 - REVISION RECEIVED ON 12/01/2022 - ACCEPTED ON 24/01/2022

DOI: 10.4244/EIJ-D-21-00970

Abbreviations

BAV	bicuspid aortic valve
CI	confidence interval
CRA	cranial
CT	computed tomography
IQR	interquartile range
LAO	left anterior oblique
LCA	left coronary artery
LCS	left coronary sinus
NL	native leaflet
OR	odds ratio
RCA	right coronary artery
RCS	right coronary sinus
TAV	tricuspid aortic valve
TAVR	transcatheter aortic valve replacement
THV	transcatheter heart valve

Introduction

Transcatheter aortic valve replacement (TAVR) has revolutionised the treatment of severe aortic stenosis and is equal or superior to surgical aortic valve replacement across the entire spectrum of surgical risk[1-4]. As TAVR indications are now expanding into lower-risk and younger patients who have a longer life expectancy, there will be an increasing need for coronary angiography or intervention after TAVR. These patients endure a high cumulative risk of progressive/unstable coronary artery disease which shares similar pathogenic or aggravating factors with aortic stenosis[5,6]. Coronary access issues may be one of the major concerns of long-term management after TAVR, because the geometric interaction between the coronary ostia and the transcatheter heart valves (THVs), as well as the tilted-up native aortic valve leaflets, may lead to difficulties in obtaining access to the coronary ostia[7,8].

Recently, several studies utilised computed tomography (CT) simulation analysis to evaluate the feasibility of coronary access after TAVR using self-expanding or balloon-expandable THVs in tricuspid aortic valve (TAV) patients. These studies indicated coronary access might be challenging in a significant proportion of the non-selected patients and explained the main mechanism of potential interferences[9-11]. However, patients with bicuspid aortic valve (BAV) were excluded from these studies, although BAV is more common than TAV in the younger aortic valve stenosis population (e.g., from 27.9% in those older than 80 years to 62.5% in those 61 to 70 years old) and the prevalence of BAV in TAVR patients is expected to considerably increase as TAVR indication expands[12,13]. Despite several theoretical perspectives, it remains unknown whether the differences between BAV versus TAV in aortic root features and interactions with THVs impact the difficulties of coronary access after TAVR[14].

This study aimed to investigate coronary access after TAVR using a self-expanding THV in patients with BAV versus TAV, based on CT simulation.

Methods

STUDY POPULATION

Between January 2014 and December 2019, consecutive patients who underwent TAVR for severe aortic stenosis using a single self-expanding VenusA-Valve (Venus Medtech) at the Department of Cardiology, West China Hospital, were screened for inclusion. Patients who did not undergo electrocardiographically-gated contrast-enhanced CT after TAVR, or whose CT image quality was inadequate, were excluded from the analysis. TAVR procedures were performed according to standard techniques, without intentionally performing commissural alignment. The study was approved by the Institutional Review Board, and written informed consent was obtained from all patients.

CT IMAGE ACQUISITION

CT image acquisition protocols are outlined in **Supplementary Appendix 1**. All images were transferred to the FluoroCT software (version 3.2, Circle Cardiovascular Imaging) for analysis.

PRE-TAVR CT ANALYSIS

Pre-TAVR CT analysis was performed according to current guidelines[15]. Based on the number of commissures (2 or 3) and the presence or absence of a raphe, we classified aortic valve morphology as follows: type 0 BAV, type 1 BAV, and TAV[16].

DESIGN FEATURES OF VENUSA-VALVE

The design features of the VenusA-Valve relevant to coronary access after TAVR are shown in **Supplementary Figure 1**. The dimensions were measured using the manufacturer's project files **(Supplementary Table 1)**. Briefly, its design is similar to that of CoreValve/Evolut (Medtronic) THVs, which are the world's most widely used self-expanding THVs. The frame is made of a network of diamond shapes consisting of alternating cells and nodes. It is wrapped with a bioprosthetic skirt between inflow and leaflet nadir levels, and hosts three bioprosthetic valve commissural posts, comprising a commissural triangle and a commissural diamond, which are also wrapped in bioprosthetic material.

POST-TAVR CT ANALYSIS AND DEFINITION

Key post-TAVR CT measurements are summarised in **Figure 1A-Figure 1I**. The distances from the left or right coronary artery (LCA/RCA) ostium to the THV inflow plane and the THV short axis were defined as ostium-inflow distance and ostium-THV distance, respectively. The ostium-commissure angle was measured between the projection of the coronary ostium midpoint onto the THV commissure plane along the long axis and its closest THV commissure. The perpendicular distance from the nadir of the left or right coronary sinus (LCS/RCS) to the THV inflow plane was measured as the THV implantation depth.

Four coronary access classifications were defined according to the interferences and the corresponding theoretical severity **(Figure 1E-Figure 1G, Central illustration A)**. If the coronary ostium faced the sealed commissural post or inner skirt, these

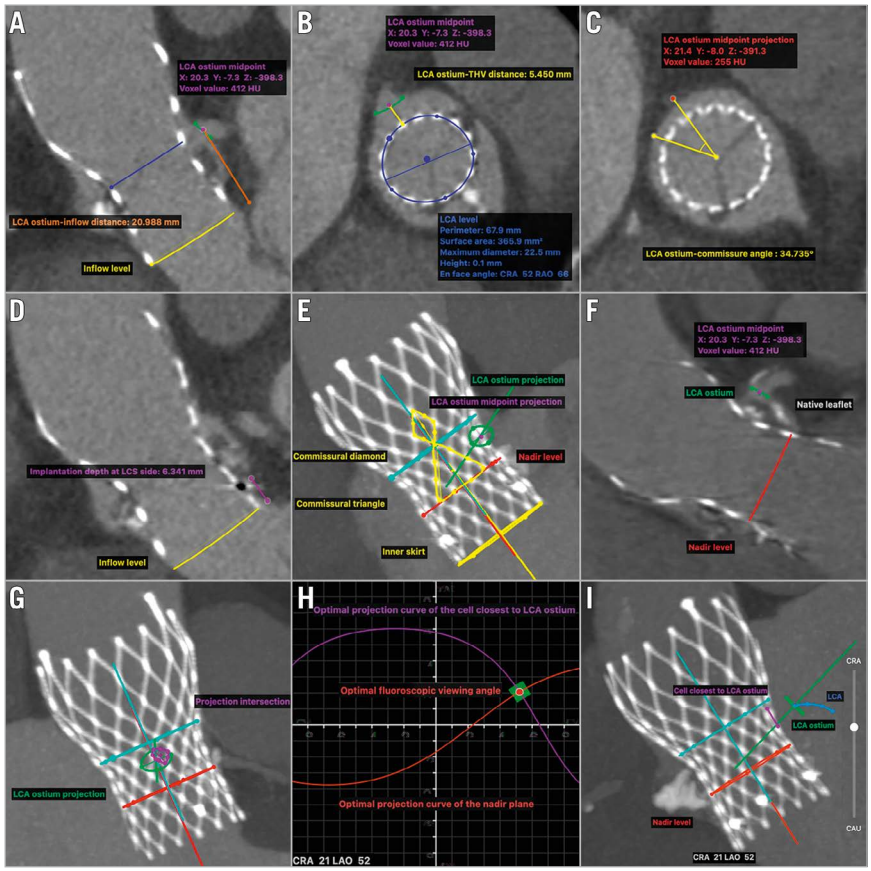

Figure 1. *Post-TAVR CT measurements of the geometric interaction between deployed THV and coronary ostia. A-D. The measurements of LCA ostium-inflow distance, LCA ostium-THV distance, LCA ostium-commissure angle, and implantation depth at LCS side, respectively. E. MIP en face view of the commissural post (yellow triangle and diamond) closest to the LCA ostium. If the ostium faced the commissural post or inner skirt, THV-related challenging LCA access was identified. F. Double-oblique long-axis plane of the THV cutting through its centreline and LCA ostium. If the ostium faced the tilted-up bulky native leaflet, NL-related challenging LCA access was identified. G. MIP en face view of LCA ostium projection onto THV long-axis plane along the direction between LCA ostium midpoint and the centre of THV short axis. If the short-axis diameter of the intersection of LCA ostium projection and the closet cell projection was less than 2 mm (cut-off value was chosen based on 6 Fr catheter size), a coaxial catheter engagement was not allowed, and THV-related complex LCA access was identified. H-I. Double-S curve method was used to calculate the optimal fluoroscopic viewing angle for LCA access, in which view the THV nadir plane and the cell closest to LCA ostium were both in plane and the ostium was nearly in plane while the THV was fully elongated. CT measurements of the geometric interaction between deployed THV and RCA ostium could be done using the same methods. CRA: cranial; CT: computed tomography; LAO: left anterior oblique; LCA: left coronary artery; LCS: left coronary sinus; MIP: maximum intensity projection; NL: native leaflet; RAO: right anterior oblique; TAVR: transcatheter aortic valve replacement; THV: transcatheter heart valve*

structures would significantly interfere with coronary engagement. We defined this as "THV-related challenging coronary access". If the coronary ostium faced the tilted-up native leaflets (NL), this would also significantly interfere with coronary engagement, and we defined this as "NL-related challenging coronary access". For non-challenging coronary access, coronary engagement may also be interfered with by the THV frame not being wrapped with bioprosthetic material. If a coaxial coronary engagement was not allowed, this was defined as "THV-related complex coronary access". Other coronary access was classified as "favourable coronary access".

We used the double S-curve method to calculate the optimal fluoroscopic viewing angle, in which the THV nadir plane and the closest cell to the coronary ostium were both in plane. The coronary ostium was also nearly in plane while the THV was fully elongated, allowing the optimal identification of the closest cell and clear identification of the coronary ostium **(Figure 1H, Figure 1I)**. However, the closest cell of challenging coronary access was wrapped in bioprosthetic material or covered by a native leaflet, and this method was not applicable. Meanwhile, due to the physical limitations of current angiography systems, extreme angulations, although optimal, may not be practical. A practical projection range described by a previous study was adopted[17].

FOLLOW-UP

During follow-up, the indication for coronary angiography or intervention was judged by a consultant cardiologist. In patients who underwent coronary access, coronary engagement was defined as

CENTRAL **ILLUSTRATION** **Coronary access after TAVR in bicuspid versus tricuspid aortic stenosis.**

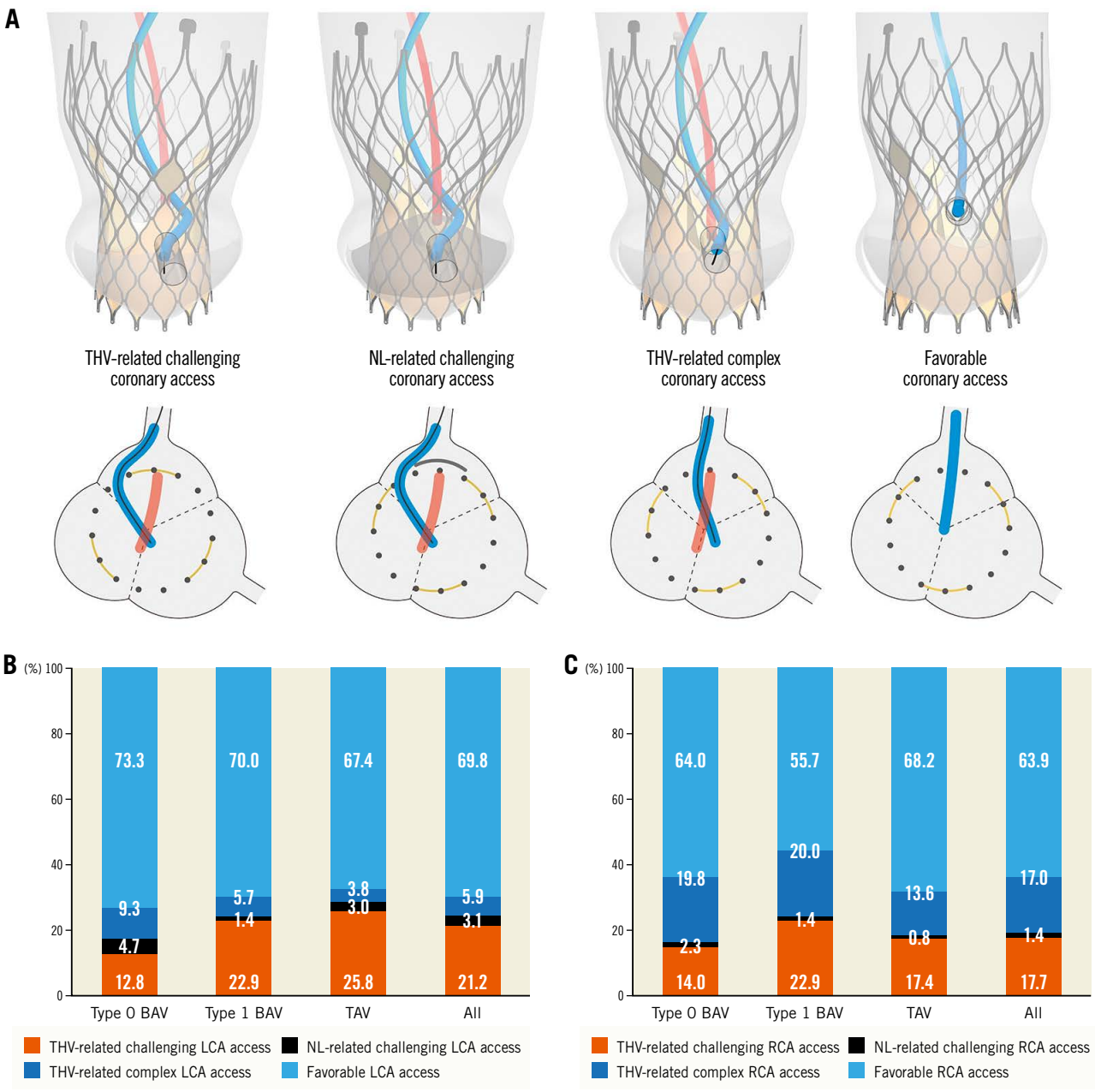

A) A graphic representation of coronary access classification examples. The yellow arcs, grey arcs, and dark grey dots indicated the cross section of the sealed commissural post, tilted-up native leaflet, and THV metallic frame, respectively. B & C) Stacked bars with the distribution of CT-identified coronary access classification stratified by native aortic valve morphology, respectively. BAV: bicuspid aortic valve; LCA: left coronary artery; NL: native (aortic valve) leaflet; RCA: right coronary artery; TAV: tricuspid aortic valve; THV: transcatheter heart valve

"unsuccessful" when it was deemed impossible to obtain selective or semi-selective cannulation.

STATISTICAL ANALYSIS

Continuous variables are presented as means±standard deviation or median (interquartile range [IQR]) and were compared using One-way Analysis of Variance or Kruskal–Wallis H tests, respectively. Categorical variables are presented as counts and percentages and were compared using the chi-square test. Bonferroni correction was utilised for *post hoc* multiple comparisons. Paired categorical data were analysed using McNemar's test. The cumulative incidence of time-to-event outcomes was estimated using the

Kaplan-Meier method. Multivariable logistic regression analysis was utilised to determine the predictors of THV-related challenging coronary access. Odds ratios (ORs) were reported with their 95% confidence intervals (CIs). Discrimination of the final model was assessed using the C-statistic. The relative importance of each predictor was measured using the partial chi-square statistic minus the predictor degree of freedom (df). A two-sided p-value of less than 0.05 was considered statistically significant. All analyses were performed using Stata 15.1 SE (StataCorp).

Results

A total of 86 type 0 BAV, 70 type 1 BAV, and 132 TAV patients were included in this study. Baseline characteristics, TAVR procedural characteristics, and in-hospital outcomes are outlined in **Supplementary Table 2**. The mean age was 73.7±7.0 years, females accounted for 46.2%, the average STS-PROM score was 6.4±4.4%, and 24.7% of patients had pre-existing coronary artery disease. Most pre-TAVR CT measurements were significantly different among groups. Particularly, LCA ostium was significantly higher in the type 0 BAV group than in the type 1 BAV or TAV group (15.4±3.7 mm vs 13.2±3.7 mm or 12.9±2.5 mm, all p<0.001); however, the difference was not observed in RCA ostium height (15.8±3.5 mm vs 14.8±3.8 mm vs 15.5±3.3 mm, p.overall=0.173).

THE GEOMETRIC INTERACTION BETWEEN DEPLOYED THV AND CORONARY OSTIA

Post-TAVR CT measurements are summarised in **Table 1**. In BAV, THVs are more likely to be implanted shallowly, especially in the type 0 BAV group (LCS side: 8.9±3.5 vs 9.9±3.4 vs 10.2±3.9 mm, p.overall=0.027; RCS side: 7.9±3.8 vs 8.6±3.9 vs 9.6±3.7 mm, p.overall=0.005). Along the THV long axis, most LCA ostia were located between the nadir and commissure levels (67.1%), while 1.0% of patients had LCA ostium below the nadir level facing the skirt, and the corresponding percentages for RCA ostium were 59.4% and 3.5%, respectively. Along the THV circumference, coronary ostia were randomly distributed without a significant difference among groups **(Supplementary Figure 2)**.

CT-IDENTIFIED CORONARY ACCESS CLASSIFICATION

The distribution patterns of CT-identified coronary access classification are outlined in **Central illustration (B, C)**.

The incidence of THV-related challenging LCA access was 21.2%, in which 17.7%, 2.4%, and 1.0% were interfered with by

Table 1. Post-TAVR MSCT measurements of the study population.

		Type 0 BAV N=86	Type 1 BAV N=70	TAV N=132	*p*.overall
THV implantation depth	Implantation depth at LCS side, mm	8.9±3.5	9.9±3.4	10.2±3.9	0.027
	Implantation depth at RCS side, mm	7.9±3.8	8.6±3.9	9.6±3.7	0.005
Relationship between LCA ostium and THV long axis	LCA ostium below THV leaflet nadir level	1 (1.2%)	0 (0.0%)	2 (1.5%)	0.006
	LCA ostium above THV commissure level	39 (45.3%)	20 (28.6%)	31 (23.5%)	
	LCA ostium between nadir and commissure levels	46 (53.5%)	50 (71.4%)	99 (75.0%)	
LCA ostium-THV distance, mm		6.7±2.8	5.6±1.9	6.1±2.2	0.012
LCA ostium-inflow distance, mm		24.3±4.3	23.5±4.0	23.3±4.4	0.217
LCA ostium-commissure (closest) angle, degree		29.7±17.5	28.0±19.4	26.6±17.7	0.488
Intersection of LCA ostium projection and closet cell projection onto THV long-axis plane	Intersected projection area, mm^2	8.7±3.5	8.1±2.7	8.5±3.1	0.404
	Intersected projection perimeter, mm	10.7±2.1	10.4±1.6	10.5±1.8	0.613
	Intersected projection LAD, mm	3.9±0.8	3.8±0.6	3.8±0.7	0.350
	Intersected projection SAD, mm	2.8±0.7	2.7±0.6	2.9±0.6	0.271
Relationship between RCA ostium and THV long axis	RCA ostium below THV leaflet nadir level	2 (2.3%)	4 (5.7%)	4 (3.0%)	0.310
	RCA ostium above THV commissure level	39 (45.3%)	22 (31.4%)	46 (34.8%)	
	RCA ostium between nadir and commissure levels	45 (52.3%)	44 (62.9%)	82 (62.1%)	
RCA ostium-THV distance, mm		6.8±2.5	6.5±2.7	6.7±2.5	0.826
RCA ostium-inflow distance, mm		24.2±4.9	23.4±4.6	23.8±5.2	0.587
RCA ostium-commissure (closest) angle, degree		32.2±17.0	26.8±16.4	29.0±16.6	0.130
Intersection of RCA ostium projection and closet cell projection onto THV long-axis plane	Intersected projection area, mm^2	6.9±3.1	7.1±3.4	8.0±3.0	0.020
	Intersected projection perimeter, mm	9.5±2.1	9.6±2.3	10.3±2.0	0.011
	Intersected projection LAD, mm	3.5±0.8	3.5±0.9	3.7±0.7	0.013
	Intersected projection SAD, mm	2.5±0.7	2.5±0.7	2.7±0.7	0.015
Coronary ostia angle, degree		136.8±39.6	113.7±27.3	137.5±24.3	<0.001

Data are expressed as mean±standard variation. BAV: bicuspid aortic valve; LAD: long-axis diameter; LCA: left coronary artery; LCS: left coronary sinus; MSCT: multislice computed tomography; RCA: right coronary artery; RCS: right coronary sinus; SAD: short-axis diameter; TAV: tricuspid aortic valve; TAVR: transcatheter aortic valve replacement; THV: transcatheter heart valve

commissural triangles, commissural diamonds, and skirts, respectively. The corresponding percentages for THV-related challenging RCA access were 17.7%, 12.2%, 2.1%, and 3.5%, respectively. Compared with the TAV group, the incidence of THV-related challenging LCA access was significantly lower in the type 0 BAV group (12.8% vs 25.8%; OR 0.42, 95% CI: 0.20-0.89), but was similar in the type 1 BAV group (22.9% vs 25.8%; OR 0.85, 95% CI: 0.43-1.69) **(Figure 2)**. No significant difference was found among groups regarding the incidence of THV-related challenging RCA access (14.0% vs 22.9% vs 17.4%). On multivariable analysis, ostium-commissure angle, implantation depth, coronary ostium height and THV size (only for LCA) were found to be the independent predictors of THV-related challenging coronary access **(Table 2)**. The final models had excellent discrimination (C-statistic: 0.96 and 0.94; respectively), and the ostium-commissure angle (X^2-df : 44.94 and 41.71, respectively) contributed most to their performance.

The incidence of NL-related challenging LCA access was 3.1%, and one patient with the LCA ostium also facing the skirt was not counted. The corresponding percentage for RCA access was 1.4%, and two patients with the RCA ostium also facing the skirt or commissural triangle were not counted. There were no significant differences among groups (4.7% vs 1.4% vs 3.0%, p.overall=0.514; 2.3% vs 1.4% vs 0.8%, p.overall=0.626; respectively).

THV-related complex LCA access was observed in 5.9% of patients, and the percentage in the BAV groups was numerically higher than in the TAV group (9.3% vs 5.7% vs 3.8%, p.overall=0.240). The incidence of THV-related complex RCA access was 17.0%, and no significant difference was found among groups (19.8% vs 20.0% vs 13.6%, p.overall=0.373). Particularly, the incidence of THV-related complex LCA access was significantly lower than that of corresponding RCA access (5.9% vs 17.0%, p<0.001).

ASSOCIATION BETWEEN CT-IDENTIFIED CORONARY ACCESS CLASSIFICATION AND UNSUCCESSFUL CORONARY ENGAGEMENT

The estimated 5-year cumulative incidence of indicated coronary access was 15.8% (95% CI: 7.3%-32.0%). After a median follow-up of 19.4 months, 17 coronary engagements in 9 patients were performed (9 for LCA, and 8 for RCA). The procedure details are presented in **Supplementary Table 3**. At engagement-level analysis, unsuccessful rates were strongly associated with CT-identified coronary access classification (THV-related challenging vs THV-related complex vs favourable coronary access: 80.0% [4/5] vs 33.3% [1/3] vs 0.0% [0/9], p.overall=0.004), and the rate of selective engagement was numerically higher in favourable LCA access than in favourable RCA access (80.0% [4/5] vs 25.0% [1/4], p=0.206).

OPTIMAL FLUOROSCOPIC VIEWING ANGLES FOR CORONARY ACCESS AFTER TAVR

Optimal fluoroscopic viewing angles for coronary access after TAVR are represented in **Figure 3**. The median optimal viewing angle was LAO (left anterior oblique) 26.1°/CRA (cranial) 14.3° (IQR: LAO 16.2°-39.5°/CRA 2.9°-25.2°) for LCA access and LAO 55.5°/CRA 35.5° (IQR: LAO 30.9°-80.0°/CRA 19.3°-41.6°) for RCA access, and the percentage of the angles within the practical range was 87.2% and 18.1%, respectively. There were significant differences in the optimal viewing angles among groups. The percentages of optimal viewing angles suitable for guiding LCA engagement were similar among groups (64.0% vs 70.0% vs 62.1%, p.overall=0.532), but those suitable for guiding RCA engagement were significantly higher in the type 0 BAV group than in the other groups (31.4% vs 4.3% vs 9.1%, p.overall<0.001) **(Supplementary Table 4)**.

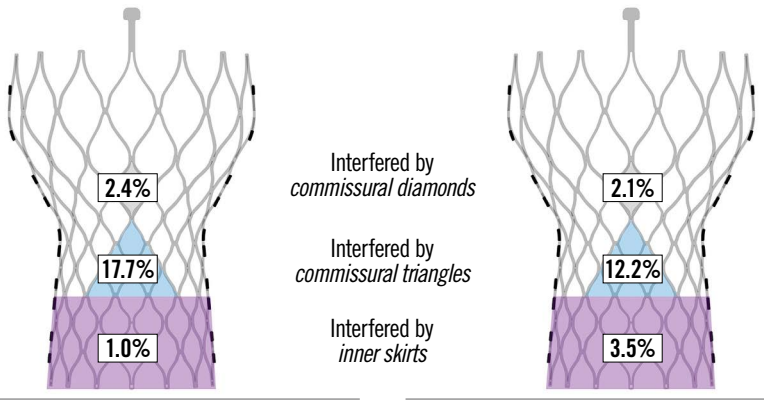

Interferences of THV-related challenging LCA access

Valve morphology	BAV Type 0	BAV Type 1	TAV
In front of inner skirt	1.2%	0.0%	1.5%
In front of commissural triangles	5.8%	22.9%	22.7%
In front of commissural diamonds	5.8%	0.0%	1.5%
All interferences	12.8%	22.9%	25.8%

Interferences of THV-related challenging RCA access

Valve morphology	BAV Type 0	BAV Type 1	TAV
In front of inner skirt	2.3%	5.7%	3.0%
In front of commissural triangles	10.5%	14.3%	12.1%
In front of commissural diamonds	1.2%	2.9%	2.3%
All interferences	14.0%	22.9%	17.4%

Figure 2. *Features of THV-related challenging coronary access according to post-TAVR CT analysis. BAV: bicuspid aortic valve; LCA: left coronary artery; RCA: right coronary artery; TAV: tricuspid aortic valve; THV: transcatheter heart valve*

Table 2. Univariable and multivariable logistic regression analysis of THV-related challenging coronary access after TAVR.

		Univariable analysis		Multivariable analysis	
		OR (95% CI)	*p*-value	OR (95% CI)	*p*-value
Predictors of THV-related challenging LCA access					
Valve morphology (TAV as control)	Type 0 BAV	0.42 (0.20-0.89)	0.023		
	Type 1 BAV	0.85 (0.43-1.69)	0.650		
LCA ostium height, mm		0.97 (0.89-1.05)	0.444	0.74 (0.63-0.88)	<0.001
THV size (23 mm as control)	26 mm	1.97 (0.82-4.77)	0.131	6.84 (1.65-28.40)	0.008
	≥29 mm	1.54 (0.59-3.98)	0.377	11.30 (2.05-62.44)	0.005
Oversizing, %		1.03 (1.00-1.06)	0.075		
THV implantation depth at LCS side, mm		0.89 (0.83-0.97)	0.006	0.62 (0.52-0.75)	<0.001
LCA ostium-commissure angle, degree		0.86 (0.83-0.90)	<0.001	0.79 (0.74-0.85)	<0.001
Predictors of THV-related challenging RCA access					
Valve morphology (TAV as control)	Type 0 BAV	0.77 (0.36-1.64)	0.496		
	Type 1 BAV	1.40 (0.69-2.87)	0.353		
RCA ostium height, mm		0.87 (0.79-0.96)	0.004	0.81 (0.71-0.92)	0.001
THV size (23 mm as control)	26 mm	1.23 (0.52-2.90)	0.644		
	≥29 mm	1.05 (0.41-2.68)	0.919		
Oversizing, %		1.05 (1.01-1.09)	0.006		
THV implantation depth at RCS side, mm		0.78 (0.71-0.86)	<0.001	0.60 (0.50-0.71)	<0.001
RCA ostium-commissure angle, degree		0.90 (0.88-0.93)	<0.001	0.84 (0.80-0.89)	<0.001

BAV: bicuspid aortic valve; CI: confidence interval; LCA: left coronary artery; LCS: left coronary sinus; OR: odds ratio; RCA: right coronary artery; RCS: right coronary sinus; TAV: tricuspid aortic valve; TAVR: transcatheter aortic valve replacement; THV: transcatheter heart valve

Discussion

To our knowledge, this is the first study to investigate coronary access after TAVR in BAV versus TAV. The main findings of this study are as follows: 1) the incidence of THV-related challenging coronary access was 21.2% for LCA and 17.7% for RCA, and type 0 BAV patients encountered fewer THV-related challenging LCA access than their TAV counterparts (OR 0.42, 95% CI: 0.20 -0.89); 2) NL-related challenging coronary access was observed in 3.1% for LCA and 1.4% for RCA, and THV-related complex coronary access was identified in 5.9% for LCA

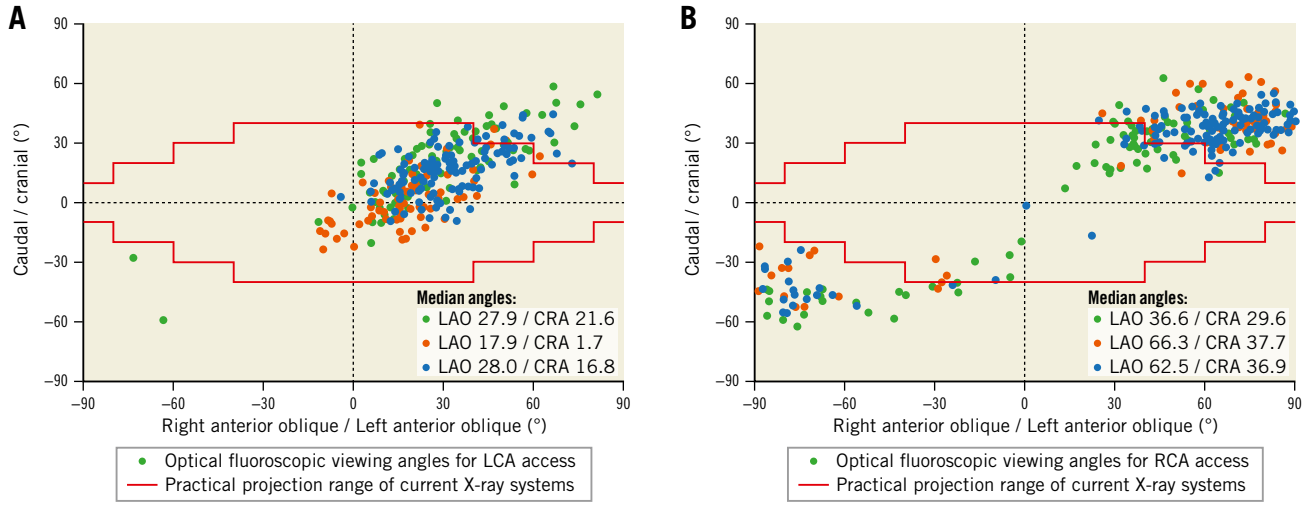

Figure 3. *Optimal fluoroscopic viewing angles for coronary access after TAVR. A, B) Scatter plots representing CT-identified individual patients' optimal fluoroscopic viewing angles for LCA and RCA access, respectively. The forest green, dark orange, and navy solid circles represent the optimal angles of patients with type 0 BAV, type 1 BAV, and TAV, respectively. The red stepped lines highlight the practical projection range of current X-ray systems. The angles between the two red stepped lines are practical. BAV: bicuspid aortic valve; LCA: left coronary artery; RCA: right coronary artery; TAV: tricuspid aortic valve; TAVR: transcatheter aortic valve replacement*

and 17.0% for RCA; however, no significant differences were found among groups; 3) the proportion of theoretical optimal fluoroscopic viewing angles that can be used to guide LCA engagement were similar among groups (64.0% vs 70.0% vs 62.1%), but those that can be used to guide RCA engagement (31.4% vs 4.3% vs 9.1%) were significantly higher in the type 0 BAV group.

Recently, several CT studies showed that the sealed commissural post and skirt were the main mechanisms of potential interference for self-expanding THVs in coronary access after TAVR and resulted in a considerable proportion of challenging coronary access; however, only TAV patients were investigated[9-11]. As the prevalence of BAV in TAVR patients is expected to increase considerably, it is also essential to elucidate the geometric interaction between the coronary ostia and the THVs in this population. Our study confirmed the findings of previous studies in both BAV and TAV patients. We further explored the independent predictors for THV-related challenging coronary access: the angle between the coronary ostium and THV commissure, THV implantation depth, coronary ostium height, and THV sizes. However, the incidence of challenging THV-related coronary access in our TAV group was lower than that reported by previous studies, except one using a very rigorous CT definition (e.g., 25.8% vs 34.8% for LCA access and 17.4% vs 25.8% for RCA access compared with the RESOLVE study). This inconsistency may be attributable to the higher THV implantation in previous studies using the repositionable Evolut system, which could achieve the optimal THV position. Interestingly, we found that type 0 BAV patients encountered fewer THV-related challenging LCA access than TAV patients (12.8% vs 25.8%), which may be explained by their anatomical feature (significantly higher LCA ostium), although there was unfavourable interaction with the THV for coronary access (higher THV implantation). These findings emphasise that the geometric interaction between the coronary ostia and the THV is influenced by the anatomical features of the aortic root.

Theoretically, the displaced bulky native leaflets may impede coronary access even if the sealed part of the THV does not interfere with the path to the coronary ostia. However, previous studies did not factor these leaflets into the prediction of the difficulty of coronary access after TAVR. This may be due to the difficulty in assessing their location and bulkiness due to their close proximity to the metallic THV frame whose blooming artefact was remarkable on CT images[9-11,18]. In this study, we found that NL-related challenging coronary access was identified in a small number of patients. A possible explanation for this discrepancy may be that the calcium burden and/or the thickness of native leaflets in our patients were much higher than in previous studies. No significant differences were observed among BAV and TAV groups regarding NL-related challenging coronary access; nevertheless, unidentified cases may also exist in this study, and the result should be interpreted with caution. Additionally, we evaluated the impact of the unwrapped metallic frame on non-challenging coronary access using a quantification method. One previous study reported that the closest vertically-aligned cell could allow selective access to the coronary ostia in non-challenging coronary access, although the cell located below or above the ostial plane may increase the difficulty[9]. However, the high rate of semi-selective coronary engagement after TAVR in the real world (12.0% - 31.7% in the RE-ACCESS study) may challenge the abovementioned viewpoint[8]. Our study showed that THV-related complex coronary access, which may significantly reduce the possibility of selective engagement, was common, especially for RCA. This may be attributable to the smaller dimensions of the RCA ostium and was consistent with the greater difficulty of RCA engagement in previous studies[8,19]. Nevertheless, there was no significant difference among the BAV and TAV groups, which indicated that this type of interference might not be associated with aortic valve morphology subtypes.

The performance of the proposed CT-identified coronary access classification for the prediction of coronary engagement difficulty was initially validated in our study, signalling that a significant proportion of patients would encounter coronary access issues after TAVR. In patients with a longer life expectancy, it may be reasonable to simplify future coronary access during the first TAVR. Theoretically, lower THV implantation can reduce the riskof THV-related challenging coronary access, but it is not an ideal option because of the increased risk of pacemaker implantation and paravalvular regurgitation, which adversely affect outcomes[20,21]. As shown in our study, the overlap between coronary ostium and THV commissure, resulting from commissural misalignment, was the most important contributor to THV-related challenging coronary access. The newly introduced promising method, aligning the THV commissures to native commissures during TAVR, may play a critical role in the simplification[22-24]. However, its usefulness may be challenged in BAV patients, especially in type 0 BAV, in which the configuration of commissures and/or the coronary takeoff angle significantly differ from those of typical TAV. Hence, this technique needs further evaluation for its feasibility in BAV patients. For patients with bulky native leaflets and low coronary ostium height, not only should the risk of coronary obstruction be considered, but the risk of challenging coronary access should also be factored into TAVR decisions. Additionally, THV designed with a low skirt, small commissural post, and large open cells can directly decrease the potential interaction. THV type selection is essential for simplification as well.

To the best of our knowledge, no study has investigated the optimal fluoroscopic viewing angles for coronary access after TAVR. The optimal projection curve, however, was widely used to provide the patient-specific coplanar view of the aortic annulus during TAVR procedures and was associated with improved outcomes[15,25]. It was also recently suggested for guiding coronary intervention in general patients[17,26]. CT simulation analysis can provide the features of the path to the coronary ostia after TAVR but using this information to guide coronary engagement requires clear identification of relevant anatomical or THV-related structures in fluoroscopic views. The optimal viewing angles may enhance feasibility, and we reported the individual optimal

viewing angles for coronary access after TAVR for the first time. We found that the theoretical optimal fluoroscopic viewing angles for coronary access after TAVR were highly variable among the type 0 BAV, type 1 BAV, and TAV groups, not all CT-identified optimal viewing angles were practical (especially for RCA access) using current C-arm equipment, and the proportion that can be used to guide RCA access was significantly higher in the type 0 BAV group. This method may further simplify coronary intervention after TAVR, but future studies are required to assess its feasibility.

Study limitations

Our study has several limitations. First, only patients undergoing TAVR with the self-expanding VenusA-Valve were included, and the results should be extrapolated with caution. However, the results may be applicable to patients receiving CoreValve/Evolut THVs whose design features are very similar to VenusA-Valve. Second, this was a retrospective single-centre study and some patients were excluded according to the predefined criteria, which may lead to selection bias. Third, the small number of coronary angiographies or intervention cases after TAVR limited the feasibility of performing complex statistical analysis. The association between the CT-identified coronary access classification and unsuccessful coronary engagement needs to be confirmed in future studies. Finally, the ability of optimal fluoroscopic viewing angles to guide coronary access was not validated, and future studies that compare its performance with the empirical method should be conducted.

Conclusions

Coronary access may be challenging or complex in a significant proportion of both BAV and TAV patients after TAVR using a self-expanding THV. Type 0 BAV anatomy may be more favourable for coronary access after TAVR. Commissural alignment techniques and THVs designed with low skirts, small commissural posts, and larger open cells may be desirable to simplify future coronary access for BAV and TAV patients during the first TAVR.

Impact on daily practice

Coronary access may be challenging or complex in a significant proportion of both bicuspid and tricuspid aortic stenosis patients after TAVR, although type 0 bicuspid aortic valve anatomy may be more favourable for post-TAVR coronary access. Commissural alignment techniques and transcatheter heart valves designed with low skirts, small commissural posts, and larger open cells may be desirable to simplify future coronary access for BAV and TAV patients during the first TAVR.

Funding

This work was supported by the National Natural Science Foundation of China (81970325, 82170375, 81901825, and 82102129); West China Hospital "1·3·5" Discipline of Excellence Project: "Percutaneous transcatheter aortic valve implantation" and "Mechanisms of aortic stenosis and the clinical applications".

Conflict of interest statement

M Chen and Y. Feng are consultants for Venus MedTech, the manufacturer of VenusA-Valve. The other authors have no conflicts of interest to declare.

References

1. Leon MB, Smith CR, Mack M, Miller DC, Moses JW, Svensson LG, Tuzcu EM, Webb JG, Fontana GP, Makkar RR, Brown DL, Block PC, Guyton RA, Pichard AD, Bavaria JE, Herrmann HC, Douglas PS, Petersen JL, Akin JJ, Anderson WN, Wang D, Pocock S; PARTNER Trial Investigators.. Transcatheter aortic-valve implantation for aortic stenosis in patients who cannot undergo surgery. *N Engl J Med.* 2010;363:1597-607.

2. Smith CR, Leon MB, Mack M, Miller DC, Moses JW, Svensson LG, Tuzcu EM, Webb JG, Fontana GP, Makkar RR, Williams M, Dewey T, Kapadia S, Babaliaros V, Thourani V, Corso P, Pichard AD, Bavaria JE, Herrmann HC, Akin JJ. Anderson WN, Wang D, Pocock SJ; PARTNER Trial Investigators.. Transcatheter versus surgical aortic-valve replacement in high-risk patients. *N Engl J Med.* 2011;364:2187-98.

3. Leon MB, Smith CR, Mack MJ, Makkar RR, Svensson LG, Kodali SK, Thourani VH, Tuzcu EM, Miller DC, Herrmann HC, Doshi D, Cohen DJ, Pichard AD, Kapadia S, Dewey T, Babaliaros V, Szeto WY, Williams MR, Kereiakes D, Zajarias A, Greason KL, Whisenant BK, Hodson RW, Moses JW, Trento A, Brown DL, Fearon WF, Pibarot P, Hahn RT, Jaber WA, Anderson WN, Alu MC, Webb JG; PARTNER 2 Investigators. Transcatheter or Surgical Aortic Valve Replacement in Intermediate-Risk Patients. *N Engl J Med.* 2016;374:1609-20.

4. Popma JJ, Deeb GM, Yakubov SJ, Mumtaz M, Gada H, O'Hair D, Bajwa T, Heiser JC, Merhi W, Kleiman NS, Askew J, Sorajja P, Rovin J, Chetcuti SJ, Adams DH, Teirstein PS, Zorn GL 3rd, Forrest JK, Tchétché D, Resar J, Walton A, Piazza N, Ramlawi B, Robinson N, Petrossian G, Gleason TG, Oh JK, Boulware MJ, Qiao H, Mugglin AS, Reardon MJ; Evolut Low Risk Trial Investigators. Transcatheter Aortic-Valve Replacement with a Self-Expanding Valve in Low-Risk Patients. *N Engl J Med.* 2019;380:1706-15.

5. Faroux L, Guimaraes L, Wintzer-Wehekind J, Junquera L, Ferreira-Neto AN, Del Val D, Muntané-Carol G, Mohammadi S, Paradis JM, Rodés-Cabau J. Coronary Artery Disease and Transcatheter Aortic Valve Replacement: JACC State-of-the-Art Review. *J Am Coll Cardiol.* 2019;74:362-72.

6. Vilalta V, Asmarats L, Ferreira-Neto AN, Maes F, de Freitas Campos Guimaraes L, Couture T, Paradis JM, Mohammadi S, Dumont E, Kalavrouziotis D, Delarochellière R, Rodés-Cabau J. Incidence, Clinical Characteristics, and Impact of Acute Coronary Syndrome Following Transcatheter Aortic Valve Replacement. *JACC Cardiovasc Interv.* 2018;11:2523-33.

7. Yudi MB, Sharma SK, Tang GHL, Kini A. Coronary Angiography and Percutaneous Coronary Intervention After Transcatheter Aortic Valve Replacement. *J Am Coll Cardiol.* 2018;71:1360-78.

8. Barbanti M, Costa G, Picci A, Criscione E, Reddavid C, Valvo R, Todaro D, Deste W, Condorelli A, Scalia M, Licciardello A, Politi G, De Luca G, Strazzieri O, Motta S, Garretto V, Veroux P, Giaquinta A, Giuffrida A, Sgroi C, Leon MB, Webb JG, Tamburino C. Coronary cannulation after transcatheter aortic valve replacement: the RE-ACCESS Study. *JACC Cardiovasc Interv.* 2020;13:2542-55.

9. Abdelghani M, Landt M, Traboulsi H, Becker B, Richardt G. Coronary Access After TAVR With a Self-Expanding Bioprosthesis: Insights From Computed Tomography. *JACC Cardiovasc Interv.* 2020;13:709-22.

10. Ochiai T, Chakravarty T, Yoon SH, Kaewkes D, Flint N, Patel V, Mahani S, Tiwana R, Sekhon N, Nakamura M, Cheng W, Makkar R. Coronary Access After TAVR. *JACC Cardiovasc Interv.* 2020;13:693-705.

11. Forrestal BJ, Case BC, Yerasi C, Shea C, Torguson R, Zhang C, Ben-Dor I, Deksissa T, Ali S, Satler LF, Shults C, Weissman G, Wang JC, Khan JM, Waksman R, Rogers T. Risk of Coronary Obstruction and Feasibility of Coronary Access After Repeat Transcatheter Aortic Valve Replacement With the Self-Expanding Evolut Valve: A Computed Tomography Simulation Study. *Circ Cardiovasc Interv.* 2020;13:e009496.

12. Roberts WC, Ko JM. Frequency by decades of unicuspid, bicuspid, and tricuspid aortic valves in adults having isolated aortic valve replacement for aortic stenosis, with or without associated aortic regurgitation. *Circulation.* 2005;111:920-5.

13. Tarantini G, Nai Fovino L, Gersh BJ. Transcatheter aortic valve implantation in lower-risk patients: what is the perspective? *Eur Heart J.* 2018;39:658-66.

14. Tarantini G, Fabris T, Cardaioli F, Nai Fovino L. Coronary Access After Transcatheter Aortic Valve Replacement in Patients With Bicuspid Aortic Valve: Lights and Shades. *JACC Cardiovasc Interv.* 2019;12:1190-1.

15. Blanke P, Weir-McCall JR, Achenbach S, Delgado V, Hausleiter J, Jilaihawi H, Marwan M, Norgaard BL, Piazza N, Schoenhagen P, Leipsic JA. Computed Tomography Imaging in the Context of Transcatheter Aortic Valve Implantation (TAVI)/Transcatheter Aortic Valve Replacement (TAVR): An Expert Consensus Document of the Society of Cardiovascular Computed Tomography. *JACC Cardiovasc Imaging.* 2019;12:1-24.

16. Sievers HH, Schmidtke C. A classification system for the bicuspid aortic valve from 304 surgical specimens. *J Thorac Cardiovasc Surg.* 2007;133:1226-33.

17. Kočka V, Thériault-Lauzier P, Xiong TY, Ben-Shoshan J, Petr R, Laboš M, Buithieu J, Mousavi N, Pilgrim T, Praz F, Overtchouk P, Beaudry JP, Spaziano M, Pelletier JP, Martucci G, Dandona S, Rinfret S, Windecker S, Leipsic J, Piazza N. Optimal Fluoroscopic Projections of Coronary Ostia and Bifurcations Defined by Computed Tomography Coronary Angiography. *JACC Cardiovasc Interv.* 2020; 13:2560-70.

18. Rogers T, Greenspun BC, Weissman G, Torguson R, Craig P, Shults C, Gordon P, Ehsan A, Wilson SR, Goncalves J, Levitt R, Hahn C, Parikh P, Bilfinger T, Butzel D, Buchanan S, Hanna N, Garrett R, Buchbinder M, Asch F, Garcia-Garcia HM, Okubagzi P, Ben-Dor I, Satler LF, Waksman R. Feasibility of Coronary Access and Aortic Valve Reintervention in Low-Risk TAVR Patients. *JACC Cardiovasc Interv.* 2020;13:726-35.

19. Faroux L, Lhermusier T, Vincent F, Nombela-Franco L, Tchétché D, Barbanti M, Abdel-Wahab M, Windecker S, Auffret V, Campanha-Borges DC, Fischer Q, Munoz-Garcia E, Trillo-Nouche R, Jorgensen T, Serra V, Toggweiler S, Tarantini G, Saia F, Durand E, Donaint P, Gutierrez-Ibanes E, Wijeysundera HC, Veiga G, Patti G, D'Ascenzo F, Moreno R, Hengstenberg C, Chamandi C, Asmarats L, Hernandez-Antolin R, Gomez-Hospital JA, Cordoba-Soriano JG, Landes U, Jimenez-Diaz VA, Cruz-Gonzalez I, Nejjari M, Roubille F, Van Belle E, Armijo G, Siddiqui S, Costa G, Elsaify S, Pilgrim T, le Breton H, Urena M, Munoz-Garcia AJ, Sondergaard L, Bach-Oller M, Fraccaro C, Eltchaninoff H, Metz D, Tamargo M, Fradejas-Sastre V, Rognoni A, Bruno F, Goliasch G, Santalo-Corcoy M, Jimenez-Mazuecos J, Webb JG, Muntané-Carol G, Paradis JM, Mangieri A, Ribeiro HB, Campelo-Parada F, Rodés-Cabau J. ST-Segment Elevation Myocardial Infarction Following Transcatheter Aortic Valve Replacement. *J Am Coll Cardiol.* 2021;77:2187-99.

20. Athappan G, Patvardhan E, Tuzcu EM, Svensson LG, Lemos PA, Fraccaro C, Tarantini G, Sinning JM, Nickenig G, Capodanno D, Tamburino C, Latib A, Colombo A, Kapadia SR. Incidence, predictors, and outcomes of aortic regurgitation after transcatheter aortic valve replacement: meta-analysis and systematic review of literature. *J Am Coll Cardiol.* 2013;61:1585-95.

21. Auffret V, Puri R, Urena M, Chamandi C, Rodriguez-Gabella T, Philippon F, Rodés-Cabau J. Conduction Disturbances After Transcatheter Aortic Valve Replacement: Current Status and Future Perspectives. *Circulation.* 2017;136:1049-69.

22. Tagliari AP, Vicentini L, Zimmermann JM, Miura M, Ferrari E, Perez D, Haager PK, Jörg L, Maisano F, Taramasso M. Transcatheter aortic valve neo-commissure alignment with the Portico system. *EuroIntervention.* 2021;17:e152-5.

23. Tang GHL, Zaid S, Fuchs A, Yamabe T, Yazdchi F, Gupta E, Ahmad H, Kofoed KF, Goldberg JB, Undemir C, Kaple RK, Shah PB, Kaneko T, Lansman SL, Khera S, Kovacic JC, Dangas GD, Lerakis S, Sharma SK, Kini A, Adams DH, Khalique OK, Hahn RT, Sondergaard L, George I, Kodali SK, De Backer O, Leon MB, Bapat VN. Alignment of Transcatheter Aortic-Valve Neo-Commissures (ALIGN TAVR): Impact on Final Valve Orientation and Coronary Artery Overlap. *JACC Cardiovasc Interv.* 2020;13:1030-42.

24. Bieliauskas G, Wong I, Bajoras V, Wang X, Kofoed KF, De Backer O, Søndergaard L. Patient-Specific Implantation Technique to Obtain Neo-Commissural Alignment with Self Expanding Transcatheter Aortic Valves: Results from the COMALIGN Study. *JACC Cardiovasc Interv.* 2021;14:2097-108.

25. Ben-Shoshan J, Alosaimi H, Lauzier PT, Pighi M, Talmor-Barkan Y, Overtchouk P, Martucci G, Spaziano M, Finkelstein A, Gada H, Piazza N. Double S-Curve Versus Cusp-Overlap Technique: Defining the Optimal Fluoroscopic Projection for TAVR With a Self-Expanding Device. *JACC Cardiovasc Interv.* 2021;14:185-94.

26. Hell MM, Schlundt C, Bittner D, Marwan M, Achenbach S. Determination of optimal fluoroscopic angulations for aorto-coronary ostial interventions from coronary computed tomography angiography. *J Cardiovasc Comput Tomogr.* 2021;15:366-71.

Supplementary data

Supplementary Appendix 1. CT image acquisition.

Supplementary Table 1. The dimensions of the VenusA-Valve.

Supplementary Table 2. Baseline, TAVR procedural characteristics, and in-hospital outcomes of the study population.

Supplementary Table 3. Procedural details of CAG or PCI after TAVR in the study population.

Supplementary Table 4. Optimal fluoroscopic viewing angles for coronary access after TAVR.

Supplementary Figure 1. The design features of the VenusA-Valve relevant to coronary access.

Supplementary Figure 2. Distribution of the position of coronary ostia in relation to THV based on post-TAVR CT analysis.

The supplementary data are published online at: https://eurointervention.pcronline.com/doi/10.4244/EIJ-D-21-00970

Supplementary data

Supplementary Appendix 1. CT image acquisition

All patients underwent electrocardiographically gated, contrast-enhanced CT before and after TAVR using a second-generation dual-source CT scanner system (Siemens SOMATOM Definition Flash; Siemens Healthcare) or a new-generation Gemstone spectral imaging CT scanner system (GE Revolution; GE Healthcare). About 80 ml iodinated contrast agent was administered intravenously, and bolus tracking with a region of interest in the ascending aorta was used. Tube potential was set to 100 to 120 kV according to the patient's body mass index, and tube current was adjusted based on the individual patient's size. Scan coverage included the aortic root and heart. Multiphasic data sets were reconstructed in 0.625 or 0.750 mm slices thickness with 50% slice overlap, and the phase with the highest image quality was chosen. Then data were transferred to a dedicated post-processing software (FluoroCT, version 3.2; Circle Cardiovascular Imaging) for analysis.

Supplementary Table 1. The dimensions of VenusA-Valve.

	23 mm THV	26 mm THV	29 mm THV	32 mm THV
Diameter at inflow level, mm	23.0	25.7	28.5	31.5
Diameter at nadir level, mm	19.5	23.2	25.1	27.7
Inner skirt height, mm	12.9	13.6	16.2	16.0
Diameter at commissure level, mm	19.7	23.2	24.9	25.9
Commissure height, mm	20.8	25.2	27.5	27.2
Frame height, mm	45.9	49.9	51.3	50.8

Detailed data were obtained by measuring the THV project files provided by the VenusA-Valve manufacturer.

Supplementary Table 2. Baseline, TAVR procedural characteristics, and in-hospital outcomes of the study population.

	Type 0 BAV N=86	Type 1 BAV N=70	TAV N=132	p.overall
Clinical characteristics				
Age, years	72.6±6.2	73.0±6.9	74.8±7.4	0.048
Female	48 (55.8%)	28 (40.0%)	57 (43.2%)	0.092
BSA, m^2	1.7±0.2	1.7±0.2	1.7±0.2	0.245
BMI, kg/m^2	22.9±3.7	22.6±4.1	22.6±3.6	0.845
Hypertension	33 (38.4%)	30 (42.9%)	65 (49.2%)	0.274
Diabetes mellitus	14 (16.3%)	10 (14.3%)	28 (21.2%)	0.418
Coronary artery disease	19 (22.1%)	12 (17.1%)	40 (30.3%)	0.095
Prior myocardial infarction	1 (1.2%)	1 (1.4%)	3 (2.3%)	1.000
Prior PCI	5 (5.8%)	2 (2.9%)	18 (13.6%)	0.019

	Type 0 BAV N=86	Type 1 BAV N=70	TAV N=132	p.overall
LM or three-vessel disease	6 (7.0%)	1 (1.4%)	3 (2.3%)	0.150
No. of diseased vessels	0.4±0.8	0.2±0.5	0.4±0.7	0.106
Cerebral arterial disease	12 (14.0%)	11 (15.7%)	26 (19.7%)	0.515
Peripheral artery disease	26 (30.2%)	20 (28.6%)	41 (31.1%)	0.935
Chronic lung disease	34 (39.5%)	25 (35.7%)	61 (46.2%)	0.316
Chronic kidney disease	26 (30.2%)	13 (18.6%)	49 (37.1%)	0.024
Prior PPI	5 (5.8%)	1 (1.4%)	3 (2.3%)	0.279
Atrial fibrillation	12 (14.0%)	13 (18.6%)	28 (21.2%)	0.401
NYHA Functional Class III/IV	74 (86.0%)	59 (84.3%)	104 (78.8%)	0.344
Estimated GFR, ml/min/1.73m^2	70.1±20.4	75.4±18.0	66.7±22.8	0.020
STS-PROM score, %	6.3±4.6	5.9±3.9	6.6±4.5	0.530
Pre-TAVR echocardiography				
LVEF, %	54.8±15.8	53.9±15.4	57.2±14.4	0.257
Peak jet velocity, m/s	5.1±0.7	4.9±0.8	4.7±0.7	<0.001
Mean gradient, mm Hg	66.2±18.5	61.5±21.4	55.4±17.7	<0.001
Moderate/severe AR	3 (3.5%)	12 (17.1%)	54 (40.9%)	<0.001
Moderate/severe MR	10 (11.6%)	12 (17.1%)	22 (16.7%)	0.530
Moderate/severe TR	5 (5.8%)	5 (7.1%)	15 (11.4%)	0.317
Pre-TAVR CT measurements				
Annulus perimeter, mm	76.4±9.2	80.0±8.5	76.1±8.7	0.007
LVOT perimeter, mm	82.9±12.9	85.7±12.2	80.7±12.3	0.028
SOV perimeter, mm	107.0±13.6	109.3±10.5	108.7±12.6	0.479
Mean SOV diameter, mm	32.5±4.7	32.4±3.0	32.3±3.6	0.949
STJ perimeter, mm	99.2±15.6	96.1±13.1	93.8±11.8	0.015
AAO perimeter, mm	133.1±15.3	130.0±17.8	120.0±17.4	0.001
LCA ostium height, mm	15.4±3.7	13.2±3.7	12.9±2.5	<0.001

	Type 0 BAV N=86	Type 1 BAV N=70	TAV N=132	p.overall
RCA ostium height, mm	15.8±3.5	14.8±3.8	15.5±3.3	0.173
Leaflet calcium volume*, mm^3	607.2±494.1	735.6±552.5	468.1±439.4	0.008
Aortic root angulation, degree	54.5±10.8	55.0±11.8	52.0±8.1	0.249
Procedural characteristics				
Conscious anaesthesia	60 (69.8%)	46 (65.7%)	99 (75.0%)	0.360
Transfemoral access	84 (97.7%)	68 (97.1%)	131 (99.2%)	0.521
Balloon predilation	84 (97.7%)	65 (92.9%)	116 (87.9%)	0.032
Coronary protection	3 (3.5%)	1 (1.4%)	11 (8.3%)	0.100
Protective stent deployment	1 (1.2%)	1 (1.4%)	6 (4.5%)	0.333
THV size				
23 mm	20 (23.3%)	10 (14.3%)	20 (15.2%)	0.369
26 mm	47 (54.7%)	34 (48.6%)	67 (50.8%)	
29 mm	18 (20.9%)	24 (34.3%)	41 (31.1%)	
32 mm	1 (1.2%)	2 (2.9%)	4 (3.0%)	
Balloon post-dilation	53 (61.6%)	42 (60.0%)	38 (28.8%)	<0.001
Device success	68 (79.1%)	60 (85.7%)	120 (90.9%)	0.047
Post-TAVR echocardiography				
LVEF, %	58.1±12.2	56.0±13.4	57.6±11.1	0.507
Peak jet velocity, m/s	2.5±0.5	2.2±0.5	2.3±0.4	0.004
Mean gradient, mm Hg	14.7±6.6	12.9±7.1	12.6±5.5	0.048
Moderate/severe AR	0 (0.0%)	2 (2.9%)	2 (1.5%)	0.276
Moderate/severe MR	4 (4.7%)	7 (10.0%)	6 (4.5%)	0.273
In-hospital outcomes				
Acute coronary occlusion	1 (1.2%)	1 (1.4%)	6 (4.5%)	0.333
Prothesis-patient mismatch	18 (20.9%)	9 (12.9%)	10 (7.6%)	0.016
Major vascular complication	2 (2.3%)	2 (2.9%)	4 (3.0%)	1.000

	Type 0 BAV N=86	Type 1 BAV N=70	TAV N=132	p.overall
Major/disabling stroke	2 (2.3%)	0 (0.0%)	1 (0.8%)	0.456
New-onset LBBB	27 (31.4%)	25 (35.7%)	55 (41.7%)	0.296
New permanent pacemaker	10 (11.6%)	16 (22.9%)	31 (23.5%)	0.076
All-cause death	1 (1.2%)	0 (0.0%)	1 (0.8%)	1.000

Data are expressed as means±standard variation or counts and percentage, as appropriate.

*The threshold was 850 HU for leaflet calcium detection.

AAO: ascending aorta; AR: aortic regurgitation; BAV: bicuspid aortic valve; BMI: body mass index; BSA: body surface area; GFR: glomerular filtration rate; LBBB: left bundle branch block;, LCA: left coronary artery; LM: left main artery; LVEF: left ventricular eject fraction; LVOT: left ventricular outflow tract; MR: mitral regurgitation; NYHA: New York Heart Association; PCI; percutaneous coronary intervention; PPI: permanent pacemaker implantation; RCA: right coronary artery; SOV: sinus of Valsalva; STJ: sinotubular junction; STS-PROM: Society of Thoracic Surgeons-Predicted Risk of Mortality; TAV: tricuspid aortic valve; TAVR: transcatheter aortic valve replacement; THV: transcatheter heart valve; TR: tricuspid regurgitation

Supplementary Table 3. Procedural details of CAG or PCI after TAVR in the study population.

Case	Age	Gender	Valve Morphology	THV Size	Time from TAVR	Procedure Indication	LCA/RCA	CAG/PCI	CT-identified Coronary Access Classification	Coronary Engagement	PCI Success
1	74 yrs	Female	Type 1 BAV	23 mm	1 day	Acute coronary occlusion	LCA	PCI	THV-related challenging coronary access	Unsuccessful	Yes
							RCA	NA	Favourable coronary access	NA	NA
2	71 yrs	Male	Type 1 BAV	29 mm	13.7 months	Chest pain	LCA	CAG	THV-related challenging coronary access	Unsuccessful	NA
							RCA	CAG	THV-related challenging coronary access	Unsuccessful	NA
3	74 yrs	Male	Type 0 BAV	26 mm	13.7 months	Stable angina	LCA	CAG	Favourable coronary access	Selective	NA
							RCA	PCI	Favourable coronary access	Selective	Yes
4	70 yrs	Male	Type 1 BAV	26 mm	14.5 months	Chest pain	LCA	CAG	Favourable coronary access	Selective	NA
							RCA	CAG	THV-related complex coronary access	Unsuccessful	NA
5	73 yrs	Male	Type 1 BAV	23 mm	16.3 months	NSTEMI	LCA	CAG	THV-related challenging coronary access	Unsuccessful	NA
							RCA	CAG	THV-related complex coronary access	Semi-selective	NA
6	70 yrs	Male	TAV	29 mm	25.0 months	Chest pain	LCA	PCI	Favourable coronary access	Selective	Yes
							RCA	CAG	THV-related complex coronary access	Semi-selective	NA
7	72 yrs	Male	Type 0 BAV	29 mm	52.7 months	Redo TAVR	LCA	CAG	Favourable coronary access	Semi-selective	NA
							RCA	CAG	Favourable coronary access	Semi-selective	NA
8	69 yrs	Female	TAV	26 mm	59.4 months	Chest pain	LCA	CAG	Favourable coronary access	Selective	NA
							RCA	CAG	Favourable coronary access	Semi-selective	NA
9	65 yrs	Female	Type 0 BAV	26 mm	62.5 months	Redo TAVR	LCA	CAG	THV-related challenging coronary access	Semi-selective	NA
							RCA	CAG	Favourable coronary access	Semi-selective	NA

BAV: bicuspid aortic valve; CAG: coronary angiography; LCA: left coronary artery; NA: not applicable; NSTEMI: non-ST segment elevation myocardial infarction; PCI: percutaneous coronary intervention; RCA: right coronary artery; TAV: tricuspid aortic valve; TAVR: transcatheter aortic valve replacement; THV: transcatheter heart valve

Supplementary Table 4. **Optimal fluoroscopic viewing angles for coronary access after TAVR.**

	Valve morphology	Optimal fluoroscopic viewing angles (median)	Optimal fluoroscopic viewing angles (interquartile range)	Within practical projection range	Within practical projection range & non-challenging access*	Within practical projection range& favourable access
LCA access	type 0 BAV (N=86)	LAO 27.9 CRA 21.6	LAO 14.4-42.3 CRA 7.4-30.4	77.9%	64.0%	55.8%
	type 1 BAV (N=70)	LAO 17.9 CRA 1.7	LAO 8.9-25.8 CAU8.2-CRA9.4	94.3%	70.0%	64.3%
	TAV (N=132)	LAO 28.0 CRA 16.8	LAO 22.1-40.9 CRA 7.1-24.3	89.4%	62.1%	59.8%
	All (N=288)	LAO 26.1 CRA 14.3	LAO 16.2-39.5 CRA 2.9-25.2	87.2%	64.6%	59.7%
RCA access	type 0 BAV (N=86)	LAO 36.6 CRA 29.6	RAO 5-LAO54 CAU 29.6-CRA29.6	36.0%	31.4%	25.6%
	type 1 BAV (N=70)	LAO 66.3 CRA 37.7	LAO 38.9-76.6 CRA25.8-44.9	5.7%	4.3%	1.4%
	TAV (N=132)	LAO 62.5 CRA 36.9	LAO 43.7-72.2 CRA 29.5-43.3	12.9%	9.1%	8.3%
	All (N=288)	LAO 55.5 CRA 35.5	LAO 30.9-80.0 CRA 19.3-41.6	18.1%	14.6%	11.8%

* Non-challenging access included THV-related complex coronary access and favourable coronary access, only in which the optimal fluoroscopic viewing angles can be used to guide coronary engagement if they were within practical projection range.

BAV: bicuspid aortic valve; CAU: caudal; CRA: cranial; LAO: left anterior oblique; LCA: left coronary artery; RAO: right anterior oblique; RCA: right coronary artery; TAV: tricuspid aortic valve; TAVR: transcatheter aortic valve replacement

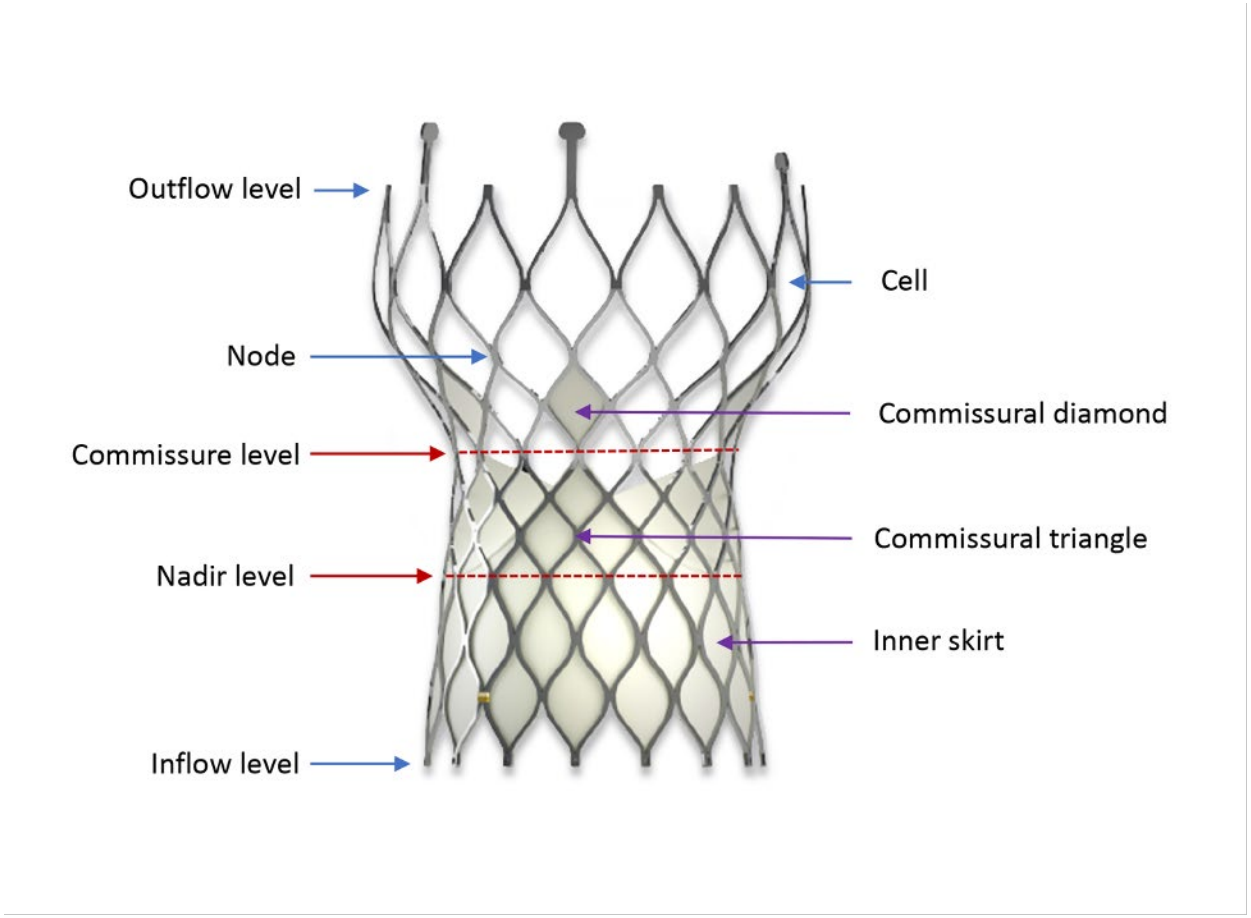

Supplementary Figure 1. The design features of the VenusA-Valve relevant to coronary access.

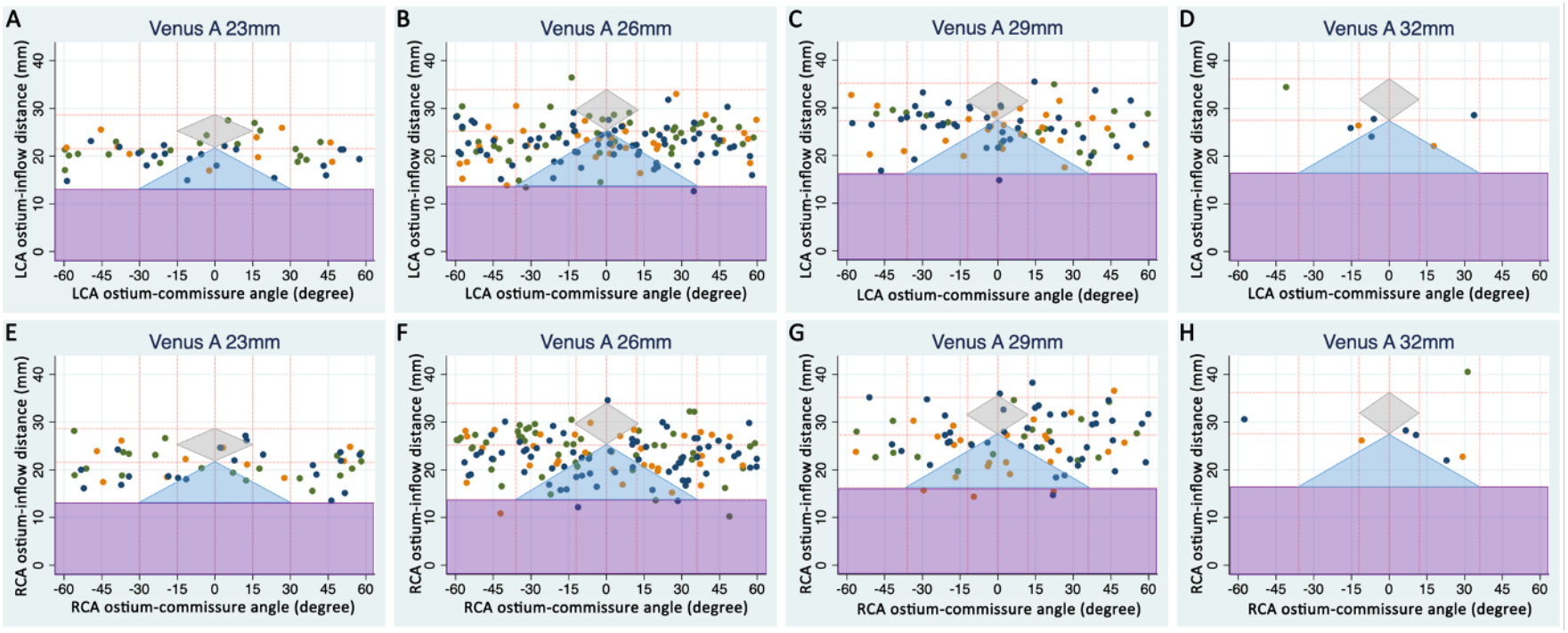

Supplementary Figure 2. Distribution of the position of coronary ostia in relation to THV based on post-TAVR CT analysis.

The light purple rectangles, light blue triangles, and light grey diamonds represented the inner skirts, commissure triangles, and commissure diamonds of the THV, respectively. The forest green, dark orange, and navy dots represented the coronary ostia of type 0 BAV, type 1 BAV, and TAV patients, respectively.
A-D and E-H showed the distribution of the position of LCA ostia and RCA ostia in relation to VenusA-Valve stratified by THV sizes, respectively.
BAV: bicuspid aortic valve; CT: computed tomography; LCA: left coronary artery; RCA: right coronary artery; THV, transcatheter heart valve; TAV: tricuspid aortic valve; TAVR: transcatheter aortic valve replacement